Spin diffusion in block copolymers as studied by pulsed NMR

Hajime Tanaka and Toshio Nishi
Department of Applied Physics, Faculty of Engineering, University of Tokyo, Bunkyo-ku, Tokyo 113, Japan
(Received 4 February 1985)

Spin diffusion in a heterogeneous polymer system, the styrene-diene—type block copolymer, has been studied using pulsed NMR. It is shown that there is a possibility the spatial dimension can be determined quantitatively from the Goldman-Shen experiment by the active use of spin diffusion. The regular structure and the small distribution of the domain sizes of block copolymers make a quantitative study possible. The possibility that the microscopic profile of the domain interface can be determined from the spin-diffusion experiment is also shown. The spatial information obtained from NMR reflects the spatial distribution of the mobility of the molecules. The spatial resolution of this technique seems to be very high because of the short-range nature of the dipole-dipole interaction. This method is nondestructive and applicable to systems for which other methods, such as transmission electron microscopy, are unsuitable.

I. INTRODUCTION

Recently an increasing amount of attention has been paid to heterogeneous systems and their interface structures. Pulsed NMR seems to be one of the most powerful methods for studying these systems.[1-4] From a pulsed NMR measurement we can obtain information on the degree of molecular motion through the spin-spin relaxation time T_2, the spin-lattice relaxation time T_1, and that in the rotating frame, $T_{1\rho}$. The spatial heterogeneity can be detected using NMR through the motional one because their origins are common.

In heterogeneous systems the NMR signal consists of two or three components, in general, and each component corresponds to each phase of the system if the mobility of the nuclei of one phase is different from that of another phase. By using this fact, the fraction of each phase can be estimated in some cases.[1-4] However, a spin-diffusion process may provide observable energy transport over a distance of several nanometers. Spin diffusion causes a loss of information on details of the morphology. This makes estimation of the fraction amounts of the phases in a heterogeneous system difficult in $T_{1\rho}$ and T_1 measurements.[5] From the above point of view, spin diffusion has been thought to be unfavorable for studying inhomogeneous systems. There is, however, the possibility that the scale of the spatial inhomogeneity can be estimated by the active use of spin diffusion, as has been pointed out by several authors.[1-14]

Block copolymers are thought to be most suitable for the purpose of checking this possibility because their morphologies are very regular[15] and we can obtain precise information on the domain size, etc., from other methods such as transmission electron microscopy (TEM), small-angle x-ray scattering (SAXS), and so on. Furthermore, the characteristic scale of inhomogeneity of these block copolymers ranges from 100 to 10000 Å, while the diffusion lengths in the case of T_1 and $T_{1\rho}$ measurements are about 100 and 10 Å, respectively.[1-3]

Furthermore, there is another important reason to study spin diffusion in block copolymers. We can study the effect of the spatial dimension on spin diffusion in block copolymers. The structures of microphase separation are grouped into three types: (1) lamellar, (2) cylindrical, and (3) spherical. We can control these morphologies through the composition of the hard segment and see the shape of the domain with TEM. In addition, we can control the domain size by varying the molecular weight without changing the composition, that is, the domain shape. As will be described, spin diffusion is strongly affected by the domain size and the spatial dimension (the degree of freedom of diffusion). Except for the micro-phase-separation structure in block copolymers, there seems to be no material with the necessary regular structure on the order of $\approx 100-1000$ Å and with a unified shape.

A few interesting studies,[8-12] using the Goldman-Shen pulse sequence,[16] have been done on spin diffusion in polymer systems, one being a crystalline polymer which is a heterogeneous system composed of crystalline lamellae and amorphous regions. Studying the structure of the crystalline polymer would be a very interesting application of spin diffusion. On the other hand, since the structure of the crystalline polymer is usually complex, it seems to be unsuitable for studying quantitatively the relation between the degree of inhomogeneity and spin diffusion. In block copolymers, T_2 for the soft segments is about 10^3 times longer than that of the hard ones, which makes the initial magnetization distribution after a $90°_{-x}$ pulse in the Goldman-Shen pulse sequence sufficiently stepwise. In other systems, such as semicrystalline polymers, there is a considerable depletion layer within the boundary of the region being selected by the Goldman-Shen pulse sequence, as pointed out by Cheung[11] and Packer *et al.*[12] Furthermore, Packer *et al.*[12] pointed out that the Goldman-Shen pulse sequence leaves magnetization in the more disordered phase in solid semicrystalline polymers and this fact has the consequence of leading to a poor signal-to-noise ratio, since the more disordered phase is usually a minority component in the signal. However, there is no such problem in block copolymers because we

can control the soft-segment fraction. From the above points of view, the block copolymer seems to be most suitable for the fundamental study of spin diffusion in various systems including materials other than polymers.

In styrene-butadiene-styrene block copolymers (SBS), Wardell *et al.*[6,7] studied the effect of spin diffusion and found that the $T_{1\rho}$ and T_1 measurements were strongly affected by spin diffusion. But their works were of a qualitative nature. In order to study spin diffusion more quantitatively, we use the Goldman-Shen pulse sequence,[16] as has been done by Assink[8] and Cheung and co-worker[9,11] in polyurethane and crystalline polymers, respectively. This is probably the first time spin diffusion in a typical block copolymer has been studied quantitatively using the Goldman-Shen pulse sequence.

II. EXPERIMENTAL

The original samples used in this experiment were typical block copolymers and are listed in Table I with their characteristics. NMR measurements were performed at 20 MHz using a Bruker PC20 proton pulsed NMR spectrometer. The NMR signals were stored in and averaged by a Kawasaki Electronica Model KR3160 transient recorder. The temperature of the samples was controlled by circulating water in the range from -30 to 80 °C. The pulse sequences used for the T_2 measurements were the solid-echo method[17] ($90°_x\tau 90°_y$) for measuring the short-T_2 component and the spin-echo method[18] [$90°_x\tau(180°_y 2\tau)_n$], Carr-Purcell-Meiboom-Gill (CPMG), for measuring the long-T_2 component to avoid the effect of inhomogeneity in the magnetic field. Both the signal from the solid echo and that from the spin echo are connected at about 150 μs by microcomputer, as described in a previous paper.[19] $T_{1\rho}$ was measured by the solid-echo-train method[20] [$90°_x\tau(90°_y 2\tau)_n$].

T_1 was measured by the modified inversion-recovery method ($180°_x\tau 90°_x\tau' 90°_y$). This pulse sequence has the advantage on obtaining the signal height just at the negative edge of the $90°_x$ pulse, which is usually difficult to determine on account of the dead time of the receiving circuit. The signal detected by this pulse sequence is shown in Fig. 1. The solid echo is formed after the $90°_y$ pulse and at a time τ' after $90°_y$ pulse (dashed line in Fig. 1), the clear peak is observed. This makes the T_1 measurement more accurate than before. We will describe the experiments using the Goldman-Shen pulse sequence later.

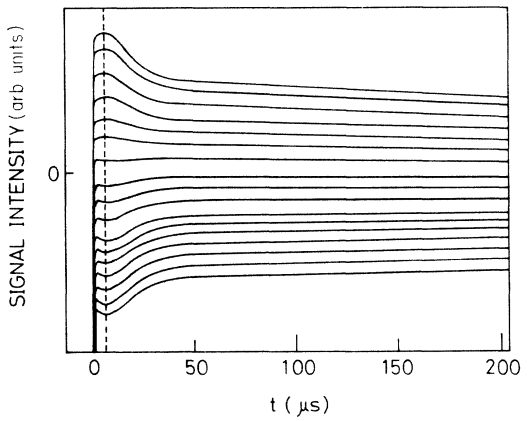

FIG. 1. Solid-echo signal after the modified inversion recovery method ($180°_x\tau 90°_x\tau' 90°_y$), with $\tau' = 5$ μs for various values of τ. τ is equal to 1, 5, 10, 15, 20, 25, 30, 40, 50, 60, 80, 100, 120, 150, 200, 300, and 1000 ms, respectively, from the bottom. The dashed line is located at time τ' after the $90°_y$ pulse, when the solid echo should have the peak.

The morphology of the block copolymer was measured with a transmission electron microscope. Observations were made using the OsO_4 or RuO_4 staining methods after being frozen by liquid N_2 and sliced into ultrathin films. The magnification factor was from 10000 to

TABLE I. Characteristics of block copolymer samples.

Sample	Type	Styrene content (wt.%)	M_w (10^4)	Plasticizer	Source
1	SB	40	8	0	Asahi Chemical Co., Ltd.
2	SBS	28	7	0	Shell Chemical Co., Ltd.
3	SBS	30	11—12	0	Shell Chemical Co., Ltd.
4	SIS	14	13	0	Shell Chemical Co., Ltd.
5	S,B radial	30	30	0	Asahi Chemical Co., Ltd.
6	S,B radial	40	14	0	Asahi Chemical Co., Ltd.
7	S,B radial	40	14		Asahi Chemical Co., Ltd.
8	SEBS	28	13	0	Shell Chemical Co., Ltd.
9	SEBS	29		0	Shell Chemical Co., Ltd.
10	SEBS Polypropylene	17		Polypropylene	Shell Chemical Co., Ltd.
11	SEBS Polypropylene	15		Polypropylene	Shell Chemical Co., Ltd.

200 000X. The shape and size of the domains were obtained from photographs.

III. RESULTS OF T_2, $T_{1\rho}$, AND T_1 MEASUREMENTS

Figures 2(a) and 2(b) are typical photographs obtained by TEM in the cases of samples 5 and 4. The morphologies of these block copolymers using TEM and their domain sizes and domain shapes are listed in Table II. It is sometimes difficult to determine clearly whether the shape of the domain is lamellar or cylindrical.

The typical result for a T_2 measurement in sample 1 is shown in Fig. 3. This is obtained by connecting the signal from the solid-echo method and that from the spin-echo (CPMG) method, as described in the previous paper.[19] After the connection, the signal is analyzed by a Pasopia 16 microcomputer (Toshiba Elect. Co., Ltd.) with the nonlinear least-squares method. The signal form is assumed to be expressed by

$$M(t)=A_1\exp\{-\tfrac{1}{2}[t/T_2(1)]^2\}+A_2\exp[-t/T_2(2)] + A_3\exp[-t/T_2(3)] , \quad (1)$$

where $M(t)$ is the transverse magnetization, t the time, A_i the amplitude of the ith component, and $T_2(i)$ the spin-spin relaxation time of the ith component. From this fitting procedure we confirm that the T_2 signal from a block copolymer is composed of three components. The fast decaying Gaussian component is from the hard segment [polystyrene (PS)], the slowly decaying one from the soft segment (rubber), and the medium one from the interface. The details of the interface detected using NMR have been described in a previous paper.[19] The thickness of the interface is estimated at about 20 Å from the pulsed NMR measurement. This interface seems to have an influence on the behavior of the spin diffusion.

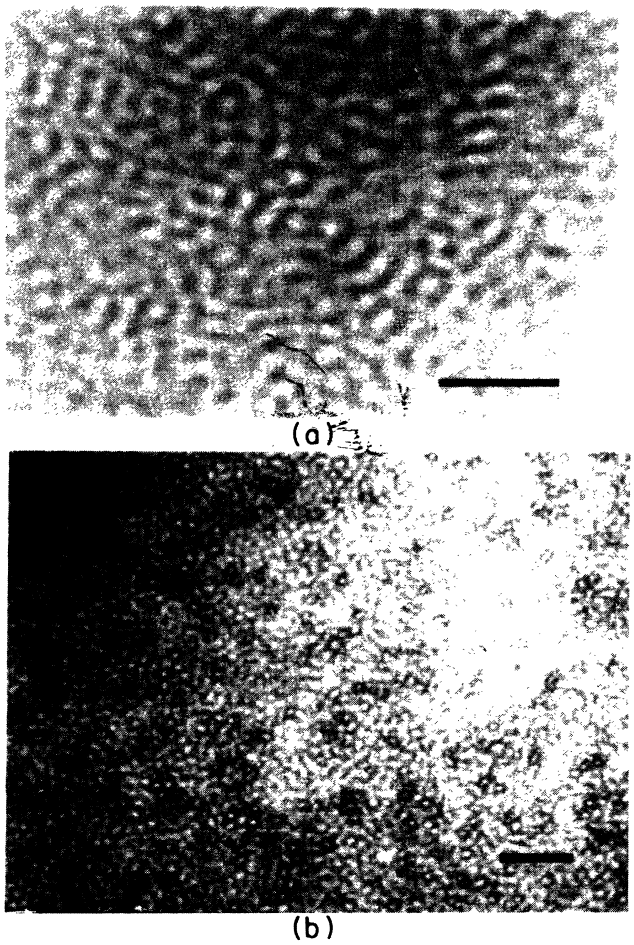

FIG. 2. Photographs of TEM observations of (a) sample 5 and (b) sample 4. The length of the black bar corresponds to 1000 Å.

TABLE II. Results of transmission electron microscopy observations.

Sample number	Domain morphology	Domain size (Å)
1	cylindrical (or lamellar)	150
2	cylindrical (or lamellar)	100
3	cylindrical (or lamellar)	120
4	spherical	200
5	cylindrical (or lamellar)	130
6	cylindrical (or lamellar)	130
7	cylindrical (or lamellar)	120
8		
9	obscure	
10	irregular	2000–8000
11	ellipsoidlike	2000–8000

The $T_{1\rho}$ measurement has been performed by the solid-echo-train method, which is the so-called $T^*_{1\rho}$. $T^*_{1\rho}$ is related to $T_{1\rho}$ by the relation[20]

$$T_{1\rho}=\lim_{\tau\to 0} T^*_{1\rho}(\tau) . \quad (2)$$

In these experiments we set $\tau=5$ μs, which seems to be short enough to assume that $T^*_{1\rho}$ is approximately equal to $T_{1\rho}$. The typical result for a $T^*_{1\rho}$ measurement in sample 1 is shown in Fig. 4. $T^*_{1\rho}$ can be analyzed by the sum of the exponential functions. In almost all cases, $T^*_{1\rho}$ is composed of two components, as shown in Fig. 4. Next, the typical result of a T_1 measurement in sample 1 is shown in Fig. 5. T_1 is almost composed of one component.

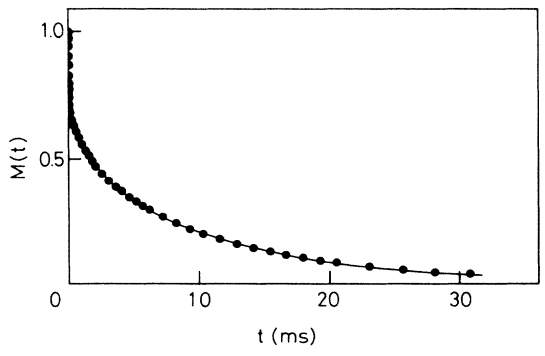

FIG. 3. T_2 signal for sample 1. The signal is composed of three components which are from the hard phase, the interface, and the soft phase.

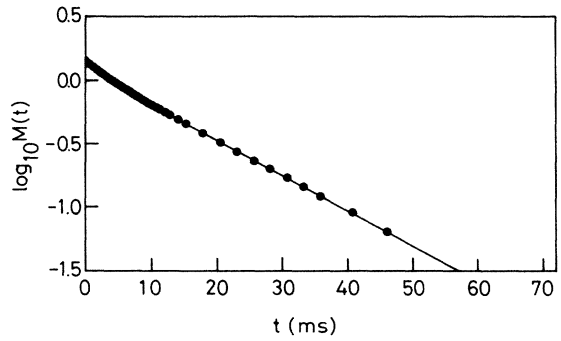

FIG. 4. $T_{1\rho}$ signal for sample 1. $\log_{10}M(t)$ is plotted against t. The signal is composed of two components.

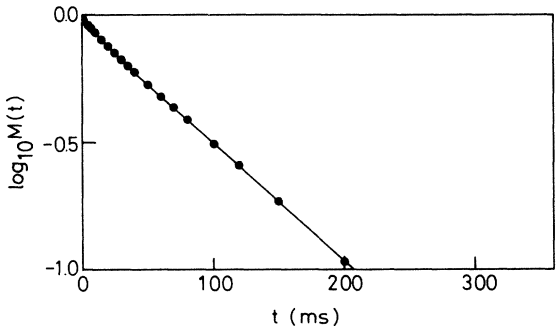

FIG. 5. T_1 signal for sample 1. $\log_{10}M(t)$ is plotted against t. The signal is almost composed of one component.

In Table III the results for all the measurements at 40°C are listed. From this table we can clearly understand the effect of spin diffusion. The number of components of signals is smaller in $T_{1\rho}$ and T_1 measurements (especially in T_1 ones) than in T_2 measurements. The results for samples 10 and 11 are different from those of the others because of their very large domain size compared to the maximum diffusive path length of spin diffusion.

IV. DISCUSSION ON THE RESULTS OF T_2, $T_{1\rho}$, and T_1 MEASUREMENTS

T_2 signals are composed of three components without the effect of spin diffusion. $T_{1\rho}$ and T_1 measurements are affected strongly by spin diffusion and the number of components decreases from $T_{1\rho}$ to T_1.

The maximum diffusive path length L is expressed[1-3,21] as $L \simeq (6Dt)^{1/2}$, where D is the spin-diffusion coefficient and t the characteristic time for diffusion. The maximum distance over which the spin diffusion is effective in the T_1 time domain is on the order of 10 nm. In the $T_{1\rho}$ measurement, L is on the order of 1 nm.[2,3]

These results are consistent with the results in Table III. The thickness of the interface is on the order of 1 nm and the domain size is on the order of 10 nm. The information on the interface, which has been successfully detected using NMR,[19] is lost in $T_{1\rho}$ measurements and that on the domain is lost in T_1 measurements, as already described. These experimental facts are consistent with the above considerations.

There is another important thing to be considered, that is, the spatial dimension in diffusion determined by the domain shape. The degree of freedom of diffusion is one, two, and three in lamellae, cylinders, and spheres, respec-

TABLE III. Results of NMR measurements (fraction amounts and relaxation time for each sample).

Sample number	$T_2(s)$			$T_{1\rho}(s)$			$T_1(s)$	
	$T_2(1)$	$T_2(2)$	$T_2(3)$	$T_{1\rho}(1)$	$T_{1\rho}(2)$	$T_{1\rho}(3)$	$T_1(1)$	$T_1(2)$
1	29%	20%	51%	18%	82%		9%	91%
	1.2×10^{-5}	1.5×10^{-3}	1.1×10^{-2}	3.6×10^{-3}	1.6×10^{-2}		2.4×10^{-2}	9.6×10^{-2}
2	19%	11%	70%	9%	91%		100%	
	1.2×10^{-5}	1.2×10^{-3}	1.8×10^{-2}	3.0×10^{-3}	2.1×10^{-2}		9.6×10^{-2}	
3	27%	15%	57%	25%	75%		100%	
	1.2×10^{-5}	1.2×10^{-3}	1.3×10^{-2}	2.2×10^{-3}	2.8×10^{-2}		1.4×10^{-1}	
4	8%	8%	84%	18%	82%		100%	
	1.3×10^{-5}	1.6×10^{-3}	1.2×10^{-2}	3.3×10^{-3}	8.7×10^{-3}		3.2×10^{-2}	
5	20%	12%	67%	25%	75%		100%	
	1.2×10^{-5}	5.0×10^{-3}	1.8×10^{-2}	2.4×10^{-3}	2.6×10^{-2}		1.3×10^{-1}	
6	28%	15%	57%	34%	66%		100%	
	1.2×10^{-5}	2.9×10^{-3}	1.5×10^{-2}	2.2×10^{-3}	2.0×10^{-2}		1.2×10^{-1}	
7	17%	28%	55%	34%	66%		10%	90%
	1.2×10^{-5}	2.7×10^{-3}	3.8×10^{-2}	3.8×10^{-3}	2.1×10^{-2}		1.4×10^{-2}	6.7×10^{-2}
8	19%	43%	38%	50%	50%		85%	15%
	1.2×10^{-5}	1.5×10^{-3}	4.5×10^{-3}	2.1×10^{-3}	5.6×10^{-3}		4.6×10^{-2}	1.2×10^{-1}
9	19%	44%	37%	44%	56%		100%	
	1.4×10^{-5}	8.5×10^{-4}	3.8×10^{-3}	1.3×10^{-3}	3.9×10^{-3}		4.2×10^{-2}	
10	25%	23%	52%	14%	64%	22%	52%	48%
	9.9×10^{-6}	8.0×10^{-4}	5.2×10^{-3}	7.9×10^{-4}	3.8×10^{-3}	1.4×10^{-2}	3.2×10^{-2}	1.1×10^{-1}
11	41%	20%	39%	14%	58%	28%	36%	64%
	9.2×10^{-6}	7.1×10^{-4}	4.5×10^{-3}	4.3×10^{-4}	2.9×10^{-2}	1.0×10^{-2}	3.2×10^{-2}	1.3×10^{-1}

tively. Taking into account the independent diffusion direction, the maximum diffusive path length should be modified as $L=(2dDt)^{1/2}$, where d is the spatial dimension of the domain.

Next we consider the effect of spin diffusion in the $T_{1\rho}$ and T_1 measurements in more detail. The temperature dependence of $T_{1\rho}$ and T_1 of PS and PB (polybutadiene) was measured by Wardell *et al.*[6,7] in their study of SBS block copolymers, which tells us that at room temperature, $T_{1\rho}(\mathrm{PB}) > T_{1\rho}(\mathrm{PS})$ and $T_1(\mathrm{PS}) > T_1(\mathrm{PB})$. In the measurement of $T_{1\rho}$ of block copolymers, the information on the interface phase is smeared out, while the information on the main two phases, a hard phase and a soft one, is not lost. But the fraction of the short $T_{1\rho}$ is different from that obtained by a T_2 measurement, and is almost equal to the sum of the hard phase and the interface. In the T_1 measurement, the information on the domain is almost lost. In a few block copolymers with very large domain sizes, such as samples 10 and 11, two components are observed in the longitudinal magnetization recovery process.

In both T_1 and $T_{1\rho}$ measurements, the decaying process of the magnetization signal is given by the following equations in the case of a system which consists of two domains, a and b, with a sharp boundary:

$$\frac{\partial M_a(\mathbf{r},t)}{\partial t}=D_a\nabla^2 M_a(\mathbf{r},t)-\frac{1}{T_a}M_a(\mathbf{r},t)\ , \tag{3}$$

$$\frac{\partial M_b(\mathbf{r},t)}{\partial t}=D_b\nabla^2 M_b(\mathbf{r},t)-\frac{1}{T_b}M_b(\mathbf{r},t)\ , \tag{4}$$

where r is the position vector, M_α the magnetization in the α domain, D_α the spin-diffusion coefficient in the α domain, and T_α the relaxation time for the α domain. T_α is equal to $T_{1\rho}$ for the α domain in the $T_{1\rho}$ experiment and to T_1 for the α domain in the T_1 and the Goldman-Shen experiments. Here the boundary conditions are

$$M_a(\mathbf{R},t)=M_b(\mathbf{R},t)\ , \tag{5}$$

$$D_a\frac{\partial M_a(\mathbf{r},t)}{\partial \mathbf{r}}\bigg|_{\mathbf{r}=\mathbf{R}}=D_b\frac{\partial M_b(\mathbf{r},t)}{\partial \mathbf{r}}\bigg|_{\mathbf{r}=\mathbf{R}}\ , \tag{6}$$

where $\mathbf{R}$ is the position vector of the interface. We observe the total magnetization M_a+M_b, where M_a is coupled with M_b by diffusion terms. The results of the calculations will be shown in a future paper.

In the case where $D_a=D_b$, the difficulty in solving the equations is reduced. The spin-diffusion coefficient is, however, proportional to the inverse of T_2. In block copolymers, T_2 for the hard segment is much shorter than that for the soft one, indicating that $D_a \gg D_b$. In our case, the approximation $D_a=D_b$ is poor and unacceptable.

Considering the spatially continuous distribution of $D(r)$ and $T(r)$, Eqs. (3) and (4) can be written generally by an equation,

$$\frac{\partial M(\mathbf{r},t)}{\partial t}=\nabla D(\mathbf{r})\nabla M(\mathbf{r},t)-\frac{1}{T(\mathbf{r})}M(\mathbf{r},t)\ , \tag{7}$$

where $T(r)$ is equal to $T_{1\rho}(r)$ in the $T_{1\rho}$ experiment and to $T_1(r)$ in the T_1 and the Goldman-Shen experiments.

In the case where the decay of the long-$T_{1\rho}$ component is slower than the spin diffusion from the phase with the short-$T_{1\rho}$ component, the observed slowly decaying component in the $T_{1\rho}$ measurement seems to reflect the spin diffusion qualitatively. This process is schematically expressed by Fig. 6. When spin diffusion is inactive, the magnetization of each phase decays independently with each relaxation time, as in limit 1 in Fig. 6. On the other hand, when spin diffusion takes place much faster than the rate of the energy flow to the lattice, the total magnetization decays exponentially with the shortest relaxation time, as in limit 2 in Fig. 6. In the intermediate cases, the behavior between the two limits is realized as shown by the solid curve in Fig. 6. In general, all processes couple with each other through Eq. (7). In the initial stage, $M(\mathbf{r}, t=0)$ is homogeneous and the diffusion is almost inactive. Therefore, the excited magnetization in the phase with the short-$T_{1\rho}$ component is first relaxed. As this process continues, the difference of the magnetization between the two regions becomes larger and the diffusion process becomes more important. In the time region after this, the relaxation and diffusion are coupled with one another in a complicated manner because of the spatial dependence of $D(r)$ and $T(r)$.

In systems such as samples 10 and 11, whose domain sizes are very large, three components were observed in the $T_{1\rho}$ measurement and two components in the T_1 measurement. In these systems, the domain size is much larger than the maximum diffusive path length, and the second term on the right-hand side of Eq. (7) is comparable to the first term.

V. A MORE QUANTITATIVE APPROACH USING THE GOLDMAN-SHEN EXPERIMENT

A. General remarks

In order to make clear the role of spin diffusion, we carried out the experiments using the Goldman-Shen

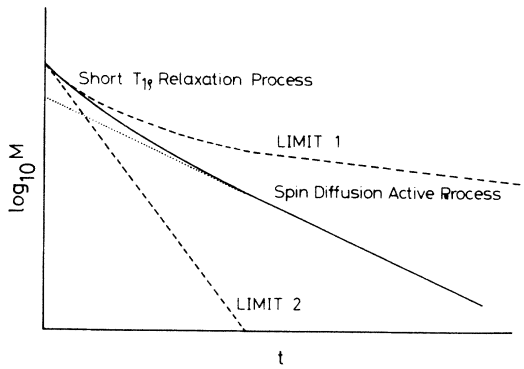

FIG. 6. Decay of the $T_{1\rho}$ signal is shown schematically for three cases. $\log_{10}M(t)$ is plotted against t. Limit 1 represents the case where the spin diffusion is inactive. In this case, the total magnetization decays with two different relaxation times characteristic to each phase. Limit 2 represents the case where spin diffusion takes place much faster than the rate of energy flow to the lattice. In this case, the magnetization decays exponentially with the shortest relaxation time in the system. The solid curve represents the intermediate case in the real system.

pulse sequence.[16] This pulse sequence can bring the spin systems with different T_2 to different spin temperatures. Therefore, when the signal is composed of more than two components, we can determine by this pulse sequence whether two-component decay is due to the heterogeneity or to the distribution of the correlation time. A few experiments using this pulse sequence have been carried out on a polyurethane[8] and a semicrystalline polymer[9,11,12] which has the heterogeneity of the amorphous and crystalline phases, but no experiment, to our knowledge, has been done on a typical block copolymer. For the purpose of studying spin diffusion quantitatively, a block copolymer is much more suitable than a crystalline polymer because the latter is complex, because of the distribution of the lamellae thickness, and the previous discussions are not in a quantitative stage, as pointed out by Cheung and Gerstein[9] and Packer *et al.*[12] In block copolymers, on the other hand, the distribution of the domain size is very small and the shape is observed clearly by TEM.

By using the Goldman-Shen pulse sequence, we can create a situation in which the magnetization of only the soft segment is excited. The difference in T_2 between a hard and soft phase of a block copolymer is much larger than that between a crystalline and an amorphous phase and those in other heterogeneous systems. For this reason the initial distribution of the magnetization after the $90°_{-x}$ pulse of the Goldman-Shen pulse sequence is sharper in block copolymers than in crystalline polymers.

The modified Goldman-Shen pulse sequence ($90°_x\tau_0 90°_{-x}\tau 90°_x\tau_1 90°_y$) used in this experiment is shown in Fig. 7. In order to avoid the dead-time effect after the pulse, we modify the original Goldman-Shen pulse sequence by the use of the solid-echo method.

During time τ_0, the magnetization in the hard segment has decayed to zero, while there is still sufficient magnetization in the soft segment. During the pulse interval τ, spin diffusion through the magnetic dipolar coupling occurs from the soft phase to the hard one, as illustrated in Fig. 8. The third $90°_x$ pulse rotates the magnetization into the transverse plane for observation and the final $90°_y$ pulse creates the solid echo. In the real experiment we replace the $90°_{-x}$ pulse with a $270°_x$ one. But this is not serious because the width of a $270°_x$ pulse is short enough (about 5 μs).

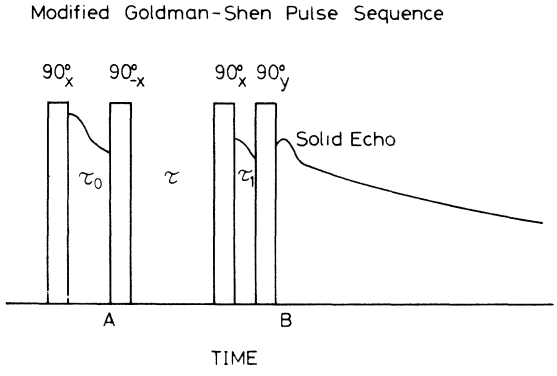

FIG. 7. Schematic figure of the modified Goldman-Shen pulse sequence ($90°_x\tau_0 90°_{-x}\tau 90°_x\tau_1 90°_y$).

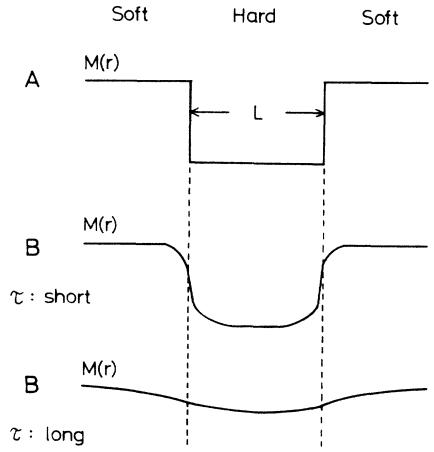

FIG. 8. Spatail distributions of the magnetization $M(r)$ are shown at times A and B, which are shown in Fig. 7. The magnetization of the hard phase is randomized in time A. L is the domain size and τ is the pulse interval in Fig. 7.

From this experiment we can estimate the domain size and the heterogeneity of inhomogeneous materials as expected from Fig. 8. When the pulse interval τ is shorter than the short-T_1 value, we need not consider the spin-lattice relaxation term. Then the problem is reduced to the pure diffusion problem. The process of spin diffusion is expressed by the following equation in such a case:

$$\frac{\partial M(\mathbf{r},t)}{\partial t} = \nabla D(\mathbf{r}) \nabla M(\mathbf{r},t) \ . \tag{8}$$

Spin-diffusion coefficient $D(r)$ is given in a regular lattice with lattice constant r_0 by[22]

$$D(r) = 0.13 r_0^2 (M_2(r))^{1/2} \ , \tag{9}$$

that is,

$$D(r) = 0.13 r_0^2 / T_2(r) \ . \tag{10}$$

From these relations $D(r)$ is directly related to $T_2(r)$. In the block copolymer, T_2 varies spatially, reflecting the domain structure. The diffusion equation with the spatially dependent diffusion coefficient is difficult to solve and the results will be presented in the future. Up to now this type of equation has not been treated and a conjecture that the diffusion constant is not so different has been made. But this assumption is quite poor for block copolymers and some semicrystalline polymers. Cheung and Gerstein[9] assumed a uniform spin-diffusion constant in some crystalline polymers. In their case, however, the difference in the values of T_2 for both phases is within less than a factor of 3 to 5. Taking into account the difference in the lattice spacing, this assumption seems to be fair.

In systems such as samples 10 and 11, which have very large domains compared to the maximum diffusive length in $T_{1\rho}$ or T_1 measurements, the second term in Eq. (7) cannot be ignored and Eq. (7) needs to be solved completely in order to analyze the experimental results. If this be-

TABLE IV. Characteristics of samples 12—15.

Designation (sample number)	Styrene content (wt.%)	M_w (10^5)	M_n (10^5)	Domain shape	Domain size (Å)
12	15	0.8	0.7	spherical	110
13	15	1.2	1.1	spherical	160
14	15	1.9	1.5	spherical	150
15	15	3.7	2.4	spherical	230

comes possible, this technique, using spin diffusion, will become applicable to the system with a large domain size, and the applicable range of this technique will become much wider.

B. Experiments using the Goldman-Shen pulse sequence and their results

Experiments using the Goldman-Shen pulse sequence were made using samples 1, 5, and 8 and samples 12—15 to make our arguments more quantitative. In the actual experiment, we used the pulse sequence $(90°_x\tau_0 270°_x \tau 90°_x \tau_1 90°_y)$. We chose the values of τ_0 and τ_1 as 50 μ and 5 μs, respectively.

Figure 9 shows the typical decaying signals after the Goldman-Shen pulse sequence is observed in sample 1 for various values of the pulse interval τ. For short τ, the recovery of the fast decaying component is clearly observed. In this early stage, we can see that almost the total magnetization is conserved. As τ becomes longer, the fast decaying component recovers gradually before at last reaching the equilibrium state. In the late stage there is the effect of the longitudinal magnetization recovery. This effect is not so serious in these block copolymers, but should be taken into account quantitatively in treating the samples with much larger domain sizes or short-T_1 values.

The molecular weight, styrene content, domain size, and domain shape of samples 12—15 are shown in Table IV. These samples have the same domain shape (that is, spherical) and three-dimensional spin diffusion occurs. These samples are suitable for studying the effect of domain size on the mobility in a hard segment, the effect of molecular weight on the interface thickness, and the effect of domain size on spin diffusion.

We measure the recovery of the magnetization as a function of τ. The results of the experiment on samples 12—15 are shown in Fig. 10. From this figure, we see that the recovery of the magnetization becomes slower as the domain size becomes larger. Since samples 13 and 14 have almost the same domain size, the recovery behavior is almost the same. From these results, we conclude that the relative accuracy in determining the domain size is almost equal to the TEM, on condition that the shape of the domain is already known and the character of the hard and soft segments are the same in various samples. Furthermore, this condition can be removed by theoretical calculation of the spin diffusion, as will be described later. From this, it is to be stressed that there is the possibility that we can estimate quantitatively the inhomogeneity of the heterogeneous systems by the use of spin diffusion in the NMR measurements.

In Fig. 11 the results on samples 1, 5, and 8 are shown. While samples 1 and 5 have almost the same domain size, their recovery behavior is very different. This is attributed to either the shape of the domain being different in these two block copolymers or the domain size obtained from TEM not reflecting the real domain structure.

The recovery of the magnetization of sample 8 is almost the same as that of sample 1. About sample 8, we cannot obtain information about the domain structure from the TEM observation because both PS and EB (ethylene-buthylene) cannot be stained by OsO_4 or RuO_4. However, we can estimate the domain size and the structure from a comparison with sample 1 by NMR measurements.

At present we cannot calculate the dependence of the recovery behavior on the spatial dimension of the domain theoretically. If this becomes possible, we will be able to estimate the shape and size of the domain only from the information obtainable by the T_2 measurements and the spin-diffusion experiments using the Goldman-Shen pulse sequence.

TABLE V. Comparison of the estimated domain size using NMR with that using TEM.

Designation (sample number)	Domain size (NMR) (Å)	Domain size (TEM) (Å)
1	130 (cylindrical)	150
5	133 (lamellar), 180 (cylindrical)	130
8	130 (cylindrical), 160 (spherical)	unobservable
12	90 (spherical)	110
13	145 (spherical)	160
14	160 (spherical)	150
15	205 (spherical)	230

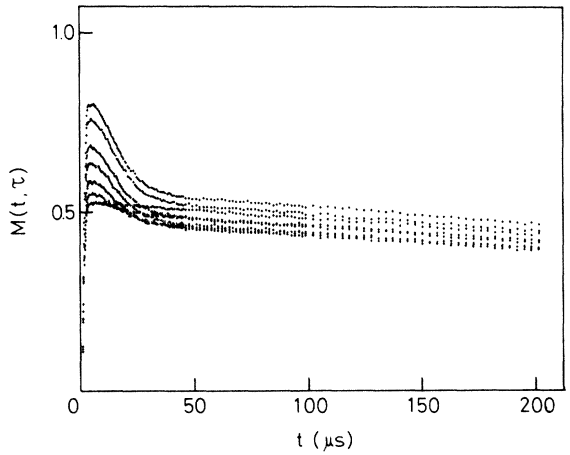

FIG. 9. Solid-echo signals after the modified Goldman-Shen pulse sequence for various values of τ. τ is equal to 1, 5, 20, 40, 70, 100, 200, and 500 ms, from the bottom, at $t=10$ μs.

C. Discussion

From the above discussion it is clear that we can obtain quantitative spatial information from the NMR measurements. Furthermore, this technique is applicable to the systems for which TEM or SAXS are not suitable, because of the lack of contrast due to no suitable staining method; or for SEBS, due to the small difference in electron density. The NMR method has the advantage that it is nondestructive and that the contrast is obtained from the difference in the mobility of the molecules.

By scaling $\tau^{1/2}$ we obtain the scaled recovery curve. The result is shown in Fig. 12. The scaling factor c is determined from the relation $\tau^{*1/2}=c\tau^{1/2}$, where τ^* is the scaled recovery time. The value of c is 1.00, 0.690, 1.00, 1.80, 1.12, 1.00, and 0.787, for samples 1, 5, 8, 12, 13, 14, and 15, respectively. All the scaled recovery curves almost coincide with each other. This indicates that there is little effect of the spatial dimension and size of the domain on the form of the recovery curve.

The maximum diffusive path length is given approximately by $(2dD\tau)^{1/2}$, where d is the spatial dimension. Therefore, the scaling factor of $1D$ and $2D$ for $3D$ is

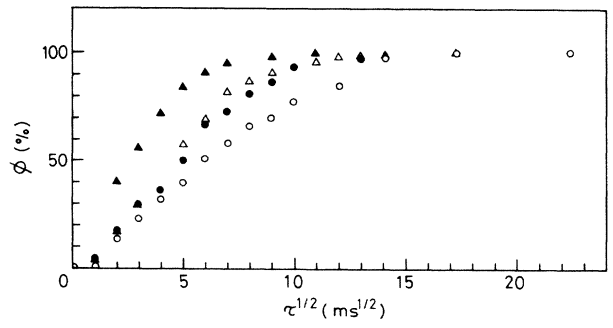

FIG. 10. Recovery of the fraction of the magnetization ϕ, with short T_2 plotted against $\tau^{1/2}$ in samples 12–15. △: sample 12, △: sample 13, ●: sample 14, and ○: sample 15.

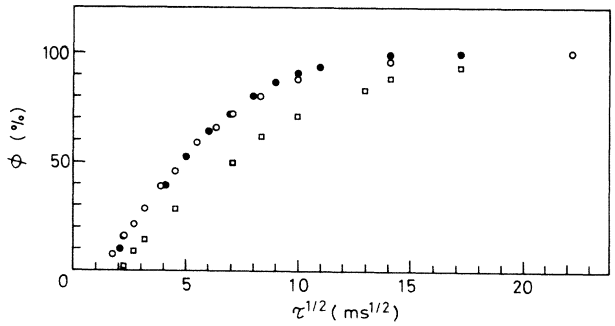

FIG. 11. Recovery of the fraction of the magnetization ϕ, with short T_2 plotted against $\tau^{1/2}$ in samples 1, 5, and 8. ○: sample 1, □: sample 5, and △: sample 8.

$(\frac{1}{3})^{1/2}$ and $(\frac{2}{3})^{1/2}$, respectively. From these considerations, $\tau^{1/2}$ should be scaled as

$$\tau^{*1/2}=\tau^{1/2}/[L/(2dD)]^{1/2} . \tag{11}$$

This is qualitatively the reasonable relation and the detailed scaling behavior needs a theoretical calculation of the spin diffusion, as already mentioned.

If this relation holds, the domain size of samples 12, 13, 14, and 15 are 90, 145, 160, and 205 Å, respectively, with the assumption that the domain size of sample 14 is equal to 160 Å. The domain size of sample 1 is 130 Å and that of sample 5 is 133 Å in the case of lamellae and 180 Å in the case of cylinders. The domain size of sample 8 is 130 Å in the case of cylinders and 160 Å in the case of spheres. The domain sizes obtained from NMR experiments are shown in Table V along with those from TEM observations. The accuracy in the determination of the domain size is rather higher in NMR measurements than in TEM observations because the photographs of bulk block copolymers using TEM are usually unclear. Furthermore, we can expect the domain shape from the comparison of both the results from NMR and from TEM. For instance, the domain shape of sample 5 seems to be lamellar, which is unclear using only TEM. In the case of sample 8, the domain shape is determined only from the NMR measurement.

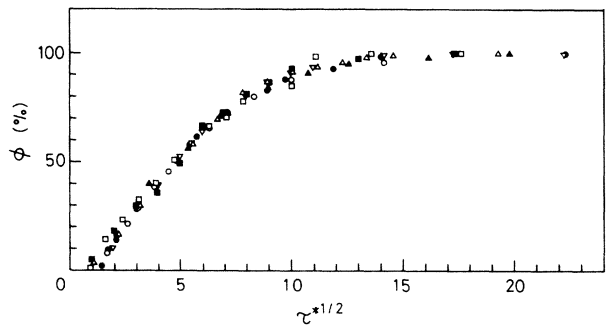

FIG. 12. Recovery of the fraction of the magnetization ϕ, with short T_2 plotted against $\tau^{*1/2}$. τ^* is scaled by the characteristic time of diffusion. ▲: sample 12, △: sample 13, ■: sample 14, □: sample 15, ○: sample 1, ●: sample 5, and ▽: sample 8.

TABLE VI. Dependence of the values of short T_2 on domain size.

Designation (sample number)	T_2 (for hard phase) (μs)	Domain size (TEM) (Å)
12	12.6	110
13	10.6	160
14	11.2	150
15	9.3	230

The domain shape can be determined by theoretical calculation of the recovery curve in the heterogeneous system. There is the possibility that $\tau^{*1/2}$ cannot be scaled easily if we take into account the dependence of the spin diffusion on the spatial dimension.

The form of the recovery curves seems to be independent of the domain shape of block copolymers, from these experiments. There are two possibilities for explaining this independence regarding domain shapes: (1) The form of the recovery curve calculated from Eq. (7) is almost independent of the degree of freedom of the spin diffusion, and (2) The spin diffusion in block copolymers has an intramolecular character and the path of the spin flip-flop is mainly along individual molecules. The former needs to be checked theoretically by solving Eq. (7) and we have no conclusion in the present stage. Equation (7) is based on the assumption that the intermolecular interaction is as active as the intramolecular one and that the system can be treated as the continuum. The validity of this assumption should be checked from the standpoint of whether the continuity can be assumed in a small domain of the order of 100 Å and whether the molecules are entangled with each other in the domain and the intermolecular interaction is sufficiently active.

Here we consider the latter possibility. In the block copolymers the molecules are arranged schematically, as shown in Fig. 13(a). All the interconnecting points are located at the interface. The propagation of the spin—flip-flop motion seems to be along the molecules, at least in the vicinity of the interface. The second moment M_2 is proportional to r_{ij}^{-6}, where r_{ij} is the distance between proton i and proton j. The spin diffusion near the interface seems to have a strong intramolecular nature on account of the short-range nature of dipole-dipole interaction. This feature is strongly affected by the molecular arrangement at the interface. At the interface the molecular arrangement is apt to be perpendicular to the interface and this makes the intramolecular character strong. The domain shape is related to the number of interconnecting points per unit volume of the domain.

The intramolecular interaction seems to be stronger than the intermolecular one in polymer systems because of the connectivity of atoms. Then, the conformation of the chains has an influence on the behavior of the spin diffusion. If the conformation and the state of packing of chains are almost independent of the domain shape, the effect of the shape on the spin diffusion is weak and the recovery curve depends only weakly on the domain shape.

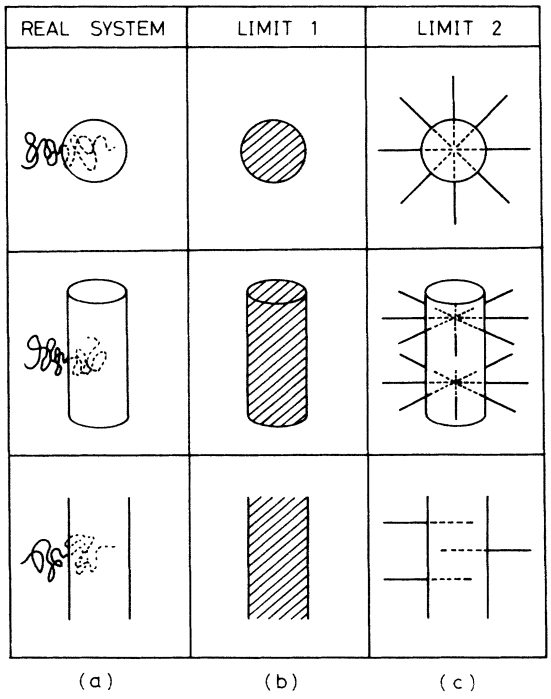

FIG. 13. Schematic representations for (a) a real block copolymer (real system), (b) the limit of the continuum model (limit 1), and (c) the opposite limit to the case of the extended and unentangled chains (limit 2).

Figures 13(b) and 13(c) represent the two limiting cases. Figure 13(b) corresponds to the continuum model in which both the intermolecular and intramolecular interactions are active in equal weight. On the other hand, Fig. 13(c) represents the limit of extended and unentangled chains, in which only the intramolecular interaction is active and the spin diffusion has a strong one-dimensional character in spite of the domain shape. In the real system [see Fig. 13(a)], the system is in the state between the two limits. By applying these considerations, we may predict the conformation and the state of packing of molecules from the comparison of spin-diffusion experiments with the calculation based on the continuum model. To check whether the continuum model is valid or not is important in applying this technique to arbitrary heterogeneous polymer systems.

Another important thing is the effect of mass diffusion. The magnetization can be transported, both by spin diffusion through the spin flip-flop due to the magnetic dipole-dipole interaction and by mass diffusion. In block copolymers the soft segment is bound to hard segments and the molecular motion is strongly reduced in soft segments. Especially in the hard phase, where the molecules are in the glassy state, there is almost no molecular diffusion. Therefore, we need not consider the effect in the present temperature region. Since these two diffusion processes have quite different temperature dependences, we can distinguish these two by measuring the temperature dependence of the diffusion constant. In the spin diffusion, the spin-diffusion constant D_S becomes smaller as

the temperature increases. On the other hand, the mass diffusion constant D_M becomes larger with a temperature increase. However, when both of these two diffusion processes are active, it is very difficult to divide them.

In the experiment using the Goldman-Shen pulse sequence, it becomes clear that the spin-spin relaxation time T_2 for the fast decaying component has a dependence on the pulse interval τ in some cases, as shown in Fig. 14. If the spatial distribution of $T_2(r)$ is like that shown in Fig. 15(a) and the initial distribution of the magnetization after a $90°_{-x}$ pulse is also as given in Fig. 15(a), the region where the magnetization first recovers, by spin diffusion from the surrounding region, has a relatively long spin-spin relaxation time compared to the center of the hard segment.

In such a case, the fast decaying component of T_2, T_2^s, after the Goldman-Shen pulse sequence, probably has the τ dependence, that is, $T_2^s(\tau)$, and $T_2^s(\tau)$ becomes shorter with an increase of τ and approaches T_2 of the PS hard segment. This type of phenomenon has been observed in the experiments on samples 12 and 1 (see Fig. 14). In general, the profile of $T_2(r)$ and that of $M(r,\tau_0)$ are not equal because

$$M(r,\tau_0)=M(r,0)\exp[-\tau_0/T_2(r)]$$

or

$$M(r,\tau_0)=M(r,0)\exp\{-\tfrac{1}{2}[\tau_0/T_2(r)]^2\}$$

are different from $T_2(r)$, as shown in Fig. 15. Therefore, there is the possibility of the dependence of T_2 on τ in general. But in the other system, $T_2(\tau)$ is almost independent of τ within experimental error. In the case of a rather sharp interface, as shown in Fig. 15(b), $T_2(\tau)$ might be independent of τ. In the case of sample 12, the interface seems to be diffuse because of the small domain size. Sample 1 is the only di-block copolymer which might be related to the dependence of T_2 on τ. The dependence is weak and careful study is required.

This type of information is very meaningful since we are able to see the more detailed profile of $T_2(r)$, as shown in Fig. 15. It cannot be obtained by other methods.

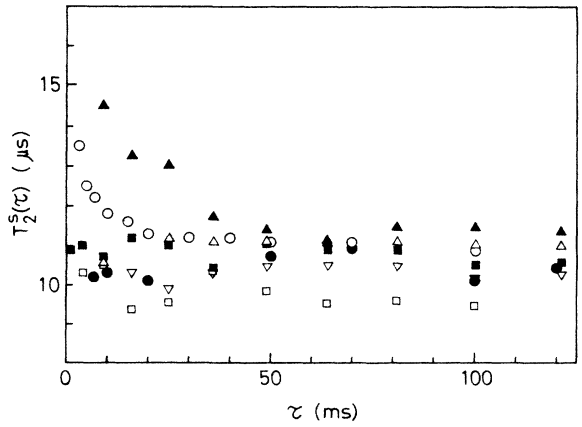

FIG. 14. Dependence of the short spin-spin relaxation time $T_2^s(\tau)$ on the pulse interval τ. Symbol identification is the same as in Fig. 12.

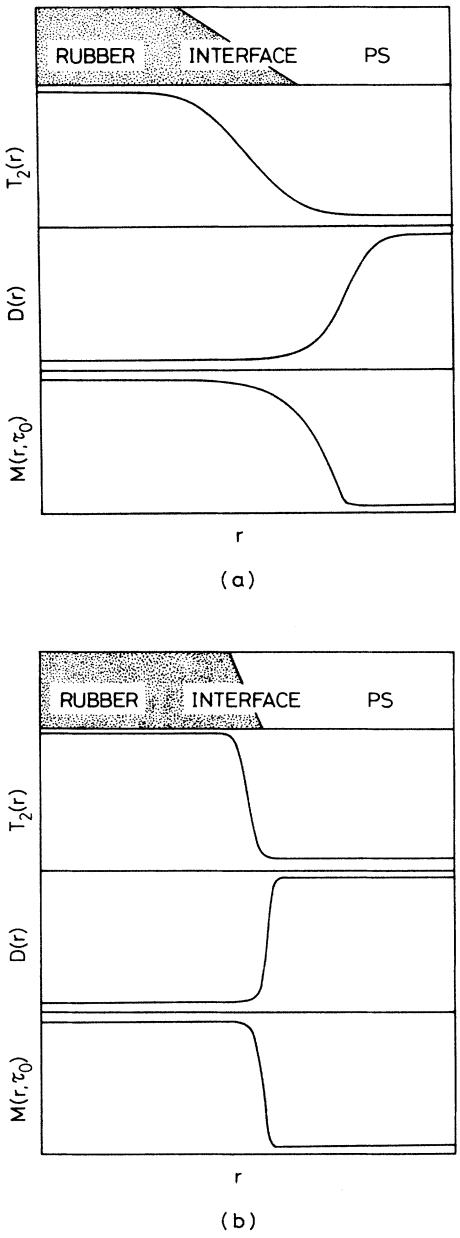

FIG. 15. Spatial profiles of the spin-spin relaxation time T_2, the spin-diffusion coefficient D, and the magnetization at time τ_0 in the Goldman-Shen pulse sequence are shown schematically as a function of r: (a) for the case of a diffusive interface, and (b) for the case of a sharp interface.

This is probably the first time in which a microscopic spatial profile of the mobility of molecules at the interface of block copolymers has been obtained. By improving the accuracy of measurement, we can estimate the profile at the interface more quantitatively. Assink[8] and Cheung[11] observed that T_2 of the slowly decaying component of the signal depend on τ. This also seems to be related to the spatial distribution of $T_2(r)$.

Cheung[11] has studied the form of the decaying curve as a function of τ_0. In our case, however, such an effect was not observed. This might be ascribed to the fact that the initial distribution of the magnetization is sharper in

block copolymers than in crystalline ones because of the large amplitude of $T_2(r)$ variation. To study this problem, it is necessary that there be no magnetization signal at all at the time just after the $90°_x$ pulse.

Next we consider the dependence of the shortest spin-spin relaxation time T_2^s on the domain size of the hard segment. In Table V, the T_2^s dependence on the domain size is shown in the case of samples 12—15, which have the same styrene content and are styrene-isoprene-styrene (SIS) triblock copolymers with different molecular weights. From Table VI, we conclude that the value of T_2^s becomes shorter as the domain size increases and finally reaches the T_2 value of bulk PS. The behavior is also observed in Table III.

This phenomenon is understood qualitatively as follows. As the domain size becomes smaller, the state of the hard segment becomes softer because the effect of interface relatively becomes larger. The mobility of PS molecules near the rubber molecules is larger than the inner part of the hard segment. This is because the two types of polymers are connected and the sharp boundary in the mobility of molecules cannot exist physically. Probably, the intermolecular effect is also active but more complicated. As the domain size becomes smaller, the state of PS molecules becomes different from the bulk property and the size effect becomes larger. This is due to both the intramolecular interaction and the intermolecular one. The behavior will be observed by measurement of the glass transition phenomenon of the hard segment. The size effect also coincides with the $T_2^s(\tau)$ dependence on τ, in the case of the small domain size.

VI. SUMMARY

The effect of spin diffusion on the results of $T_{1\rho}$ and T_1 measurements in block copolymers has been studied. A quantitative study of the heterogeneity of the block copolymers has been done using the Goldman-Shen pulse sequence. It becomes clear that this type of study makes it possible to determine quantitatively the spatial dimension of the domain. We have succeeded in determining from NMR measurements the domain size of the styrene-diene block copolymers which is consistent with the results of the TEM observations. The forms of the magnetization recovery curves in the Goldman-Shen experiments are shown to be equal to one another and all the curves can be scaled to one universal curve. The origin of this universality is briefly discussed and further theoretical work is necessary for a conclusion.

Furthermore, in a few cases we have succeeded in observing the dependence of the value of T_2 for hard phases on the interval τ in the Goldman-Shen pulse sequence. This seems to reflect the spatial profile of the interface. There is the possibility that we can estimate the spatial distribution of $T_2(r)$ at the interface by using this fact. This gives important information in studying the interface of the heterogeneous systems. This type of direct observation of the interface profile is unique to the NMR measurements.

From these studies, we confirm that there is a possibility that quantitative spatial information can be obtained from temporal information using pulsed NMR. For this purpose, a good estimation of the spin-diffusion coefficient is essential. This technique is widely applicable to various systems, such as polymer systems, biological systems, composite materials, and so on. The characteristic feature of this method is that we can obtain spatial inhomogeneity from the difference in the mobility of molecules. This differentiates this method from other methods such as TEM, SAXS, and so on, which makes it applicable to systems for which the contrast is insufficient for these other methods, because of the lack of a suitable staining method or a large enough difference in the electron density, etc. Another merit of our method is its nondestructive character.

ACKNOWLEDGMENTS

The authors are greatly indebted to the Japan Synthetic Rubber Co., Ltd. and Bridgestone Co., Ltd. for providing us with the TEM photographs of block copolymers. The authors would like to thank Dr. Shibashi of the Japan Synthetic Rubber Co., Ltd. for kindly providing us samples of styrene-isoprene-styrene triblock copolymers. This work was supported in past by a grant-in-aid from the Ministry of Education, Science and Culture, Japan.

[1]A. Abragam and M. Goldman, *Nuclear Magnetism: Order and Disorder* (Oxford University Press, New York, 1982).
[2]V. J. McBrierty, and D. C. Douglass, J. Polym. Sci., Macromol. Rev. **16**, 295 (1981).
[3]V. J. McBrierty and D. C. Douglass, Phys. Rep. **63**, 63 (1980).
[4]D. C. Douglass and V. J. McBrierty, Polym. Eng. Sci. **19**, 1054 (1979).
[5]D. C. Douglass and V. J. McBrierty, J. Chem. Phys. **54**, 4085 (1971).
[6]G. E. Wardell, V. J. McBrierty, and D. C. Douglass, J. Appl. Phys. **45**, 3441 (1974).
[7]G. E. Wardell, D. C. Douglass, and V. J. McBrierty, Polymer **17**, 41 (1976).
[8]R. A. Assink, Macromolecules **11**, 1233 (1978).
[9]T. T. P. Cheung and B. C. Gerstein, J. Appl. Phys. **52**, 5517 (1981).
[10]T. T. P. Cheung, Phys. Rev. B **23**, 1404 (1981).
[11]T. T. P. Cheung, J. Chem. Phys. **76**, 1248 (1982).
[12]K. J. Packer, J. M. Pope, R. R. Yeung, and M. E. A. Cudby, J. Polym. Sci., Polym. Phys. **22**, 589 (1984).
[13]H. Tanaka, Y. Sumi, and T. Nishi, Rep. Prog. Polym. Phys. Jpn. **27**, 545 (1984).
[14]H. Tanaka and T. Nishi, Polym. Prepr. Jpn. **33**, 2295 (1984).
[15]T. Inoue, T. Soen, T. Hashimoto, and H. Kawai, J. Polym. Sci. Part A-2, **7**, 1283 (1969).
[16]M. Goldman and L. Shen, Phys. Rev. **144**, 321 (1966).
[17]J. G. Powles and J. H. Strange, Proc. Phys. Soc. London **82**, 6 (1963).
[18]S. Meiboom and D. Gill, Rev. Sci. Instrum. **29**, 688 (1958).
[19]H. Tanaka and T. Nishi, J. Chem. Phys. **82**, 4326 (1985).
[20]J. S. Waugh and C. H. Wang, Phys. Rev. **162**, 209 (1967).
[21]N. Bloembergen, Physica **15**, 386 (1949).
[22]T. T. P. Cheung, B. C. Gerstein, L. M. Ryan, R. E. Taylor, and C. R. Dybowski, J. Chem. Phys. **73**, 6059 (1980).

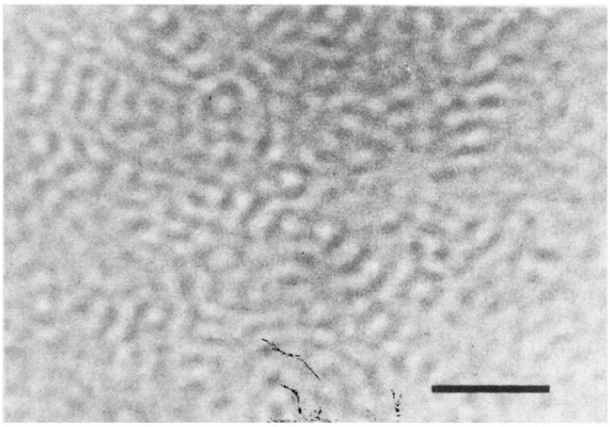

(a)

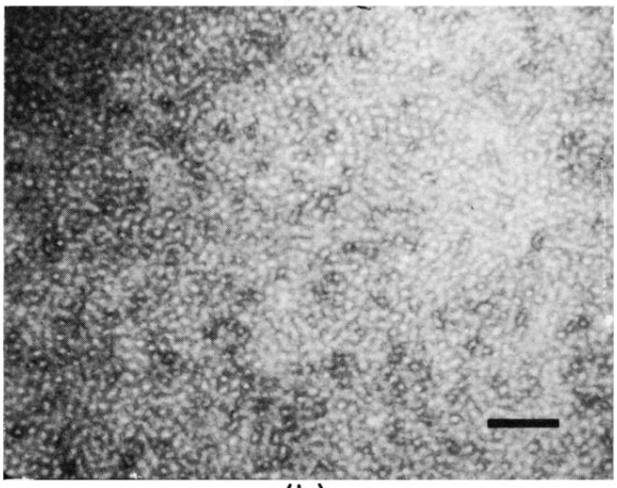

(b)

FIG. 2. Photographs of TEM observations of (a) sample 5 and (b) sample 4. The length of the black bar corresponds to 1000 Å.